Dynamic Behaviour of Differentially Steered Mobile Robot

František Dušek [1)], Daniel Honc [2)], and Rahul Sharma [3)]
Department of Process Control, Faculty of Electrical Engineering and Informatics,
University of Pardubice, Czech Republic
[1)] *frantisek.dusek@upce.cz,* [2)] *daniel.honc @upce.cz,* [3)] *rahul.sharma@student.upce.cz*

Abstract — **This article is aimed at obtaining a description of the behaviour of an ideal differentially steered drive system (mobile robot) and planar motion. The mathematical dynamic model describing the motion (speed and direction) of one robot's point is created based on the first principles approach. The trajectory of this point is converted to trajectories of wheel contact points with the plane of motion. The dynamic behaviour of motors and chassis, form of coupling between motors and wheels and basic geometric dimensions are taken into account. The resulting trajectory depends on the supply voltage of both drive motors. The dynamic model will be used for design and verification of a robot's motion control in MATLAB / SIMULINK simulation environment.**

Keywords — Dynamic system modelling, intelligent control, mobile robot.

I. Introduction

The paper deals with a dynamic model of an ideal mobile robot with differentially steered drive system and planar motion. A single-axle chassis or caterpillar chassis is mostly used in case of small mobile robots [1]. A caster wheel is added to a single-axle to ensure stability. This solution together with the independent wheel actuation allows excellent mobility on the contrary to a classic chassis – see a commercially available robot in Fig. 1. The derived mathematical model comes from lay-out, nominal geometric dimensions and other features of that robot with view of ideal behaviour of individual components and some simplifying assumptions. The aim is to create a model based on forces caused by motor torques of independent wheel drives. The model will consist of dynamic behaviour description of the chassis and DC series motors. The presented motion model based on centre of mass (primary element) dynamics is different from models reflecting kinematics only and commonly used in literature – published e.g. in [2] or [3]. Standard models describe robot's trajectory time evaluation depending on known wheel speed (information from wheel speed sensors) and chassis geometry – odometry – published e.g. in [4] Our model extends standard model with dynamic part describing wheel speed dependency on the motor supply voltage by respecting dynamics, construction, geometry and other parameters of the chassis and motors.

The motor supply voltage actuating the wheel causes driving torque and thereby wheel rotation. Inertial and resistance forces act against the driving torque. Both driving torques influence each other because of these forces. The planar curvilinear motion of the robot is result of various time variant wheel rotation speeds.

The planar curvilinear motion can be decomposed to a sum of linear (translational) and rotational motions. Force balance is the starting point for the derivation of motion equations. If F is actual force acting to a mass point with mass m and distance r from the axis of rotation then it holds for a general curvilinear motion that vector sum of all forces acting to a selected point is zero – see literature [5].

$$\vec{F} + \underbrace{m\frac{d\vec{v}}{dt}}_{\text{inertial force}} + \underbrace{m\frac{d\vec{\omega}}{dt}\times r}_{\text{Euler's force}} + \underbrace{2m\vec{\omega}\times\frac{d\vec{r}}{dt}}_{\text{Coriolis force}} + \underbrace{m\vec{\omega}\times\left(\vec{\omega}\times\vec{r}\right)}_{\text{centrifugal force}} = 0 \tag{1}$$

Application of this general equation requires specification of individual forces according to actual conditions and/or eventually implementing other acting forces. We will consider forces originated by the motion of real body – induced with resistances (losses) in addition to curvilinear motion forces.

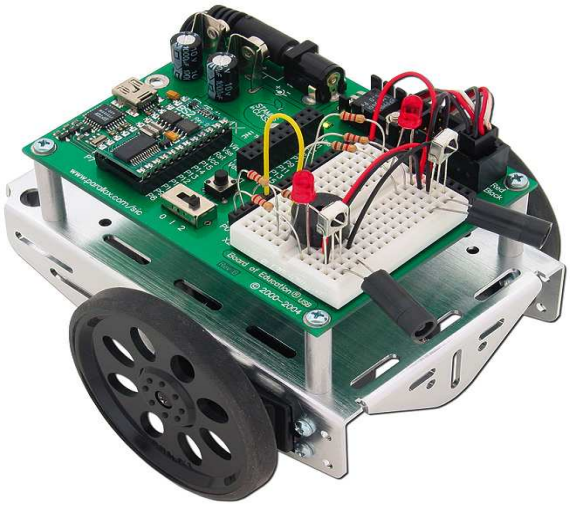

Fig. 1. Differentially steered mobile robot.

We will approximate these forces in the simplest manner to be proportional to a speed. Equations describing dependences of linear and angular velocities of the reference chassis point to actual wheel motor voltages will be result of the dynamic part.

Selection of the point where actual translation and rotation speeds will be evaluated influences significantly initial equations and hence complexity of the resulting

model. If the reference chassis point is at the centre of gravity then initial equations of the dynamic part are the simplest but equations describing dependencies between wheel speeds and linear and angular velocities are more complicated. The centre of the axis joining the wheels is the most common reference chassis point in literature. Such a choice leads to the simplest recalculation of actual wheel speeds to motion equations of that point. Trade-off between these two approaches is chosen in our paper – point at the centre of gravity projection to the axis joining the wheels is selected. A tTrajectory (time course) computation of another chassis points (points where wheels meet the ground) supplements the dynamic part of the model.

II. Mathematical Model

The described mobile robot is driven by two DC motors with common voltage source and independent control of each motor. The motors are connected with the driving wheels through a gear-box with constant gear ratio. An ideal gear-box means that it reduces linearly angular velocity and boosts the torque (nonlinearities are not considered). Losses in the motor and also in the gear-box are proportional to the rotational speed. The chassis is equipped with the caster wheel with no influence on the chassis motion (its influence is included in resistance coefficients acting against motion).

The model of the robot consists of three relatively independent parts. Description of the ideal DC series motors is given in section A. Two equations describe dependency of the motor rotation speed and current on the power supply voltage and loading torque are related to chassis dynamics. Motion equations are presented in section B – dependency between linear and angular velocities of the reference chassis point on torques acting on driving wheels. Section C is dedicated to equations describing how the motor speed influences translation and rotation speeds of the selected point and to complete model formulation. In the last Section D, the model is transformed to a simpler form which is more suitable for next using and for trajectory of an arbitrary point calculation. Equations describing trajectory corresponding to the contact points of the driving and caster wheels with the ground are formulated.

A. DC Series Motor Dynamics

An equivalent circuit of an ideal DC series motor [6] is in Fig. 2. It consists of resistance R, inductance L and magnetic field of the motor *M*. The commutator is not considered. The rotor produces electric voltage with reverse polarity than the source voltage – electromotive force, which is proportional to the rotor angular velocity ω. The torque of the rotor M_M is proportional to the current *i*.

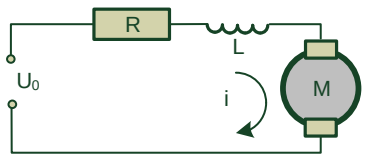

Fig. 2. Equivalent circuit of motor.

Ideal behaviour means that whole electric energy used for magnetic field creating is transformed without any losses to mechanical energy – torque of the motor. We do not consider losses in the magnetic field but only electric losses in winding and mechanical losses proportional to the rotor speed.

First equation describes motor behaviour through balancing of voltages (Kirchhoff's laws)

$$Ri + L\frac{di}{dt} = U_0 - K\omega \tag{2}$$

where

R	[Ω] is motor winding resistance,
L	[H] is motor inductance,
K	[kg.m^2.s^{-2}.A^{-1}] is back EMF constant,
U_0	[V] is source voltage,
ω	[rad.s^{-1}] is rotor angular velocity and
i	[A] is current flowing through winding.

Second equation is balance of torques (electric energy) – moment of inertia M_s, rotation resistance proportional to the rotation speed (mechanical losses) M_o, load torque of the motor M_x and torque M_M caused by the magnetic field which is proportional to current

$$M_s + M_o + M_x = M_M$$
$$J\frac{d\omega}{dt} + k_r\omega + M_x = Ki \tag{3}$$

where

J	[kg.m^2] is moment of inertia,
k_r	[kg.m^2.s^{-1}] is coefficient of rotation resistance,
M_x	[kg.m^2.s^{-2}] is load torque.

B. Chassis Dynamics

Chassis dynamics is defined by the vector of linear velocity v_B acting on the reference chassis point and with rotation of this vector with angular velocity ω_B (constant for all chassis points). It is possible to calculate the trajectory of arbitrary chassis point from these variables. The point B for which the equations are derived is the centre of gravity normal projection to the axis joining the wheels – see Fig. 3. This leads, according to the authors, to the simplest set of equation for the whole model. We consider the general centre of gravity T position – usually it is placed to the centre of the join between wheels.

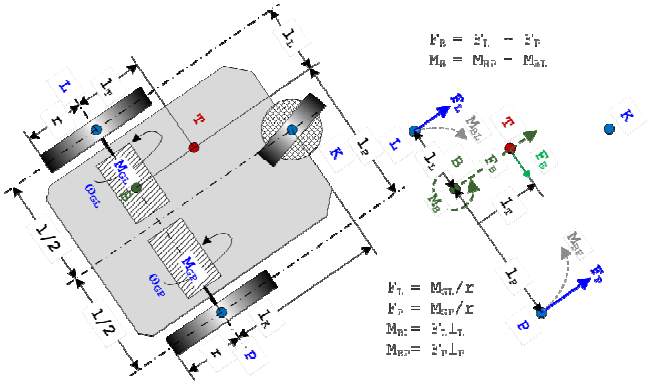

Fig. 3. Chassis diagram and forces.

We consider forces balances as starting equations. It is possible to replace two forces F_L and F_P acting to chassis in left (L) and right (P) wheel ground contact points with one force F_B and torsion torque M_B acting in point B. The

chassis is characterized with radius of the driving wheels r, total mass m, moment of inertia J_T with respect to the centre of gravity located parameters l_T, l_L, l_P.

Let us specify equation (1) for our case. The position of the centre of gravity is constant with respect to the axis of rotation so we do not need to consider Coriolis force. Similarly we do not consider the centrifugal force – chassis is supposed to be solid body represented as a point mass (centre of gravity). Because the force vector causing the movement acts in the point B and goes through the centre of gravity it is enough if we consider the inertial force by linear motion. At a rotational motion it is necessary to consider torque caused by Euler's force because the axis of rotation does not go through the centre of gravity.

By the balance of forces causing linear motion we will consider forces F_L, F_P caused by the drives, inertial force F_S and resistance force F_O which is proportional to speed v_B. The balance of forces influencing linear motion is

$$F_L + F_P + F_O + F_S = 0$$
$$\frac{M_{GL}}{r} + \frac{M_{GP}}{r} - k_v v_B - m\frac{dv_B}{dt} = 0 \tag{4}$$

where

m [kg] is robot mass,

k_v [kg.s^{-1}] is resistance coefficient against linear motion,

M_{GL} [kg.m^2.s^{-2}] is torque of the left drive,

M_{GP} [kg.m^2.s^{-2}] is torque of the right drive,

v_B [m.s^{-1}] is linear velocity and

r [m] is radius of the wheels.

The balance of torques is slightly more complicated because the rotation axis does not lie in the centre of gravity. That's why it is necessary to take into consideration not only chassis momentum M_T, but also torque $M_E = l_T F_E$ caused by Euler's force F_E. Similarly as at a linear motion we will consider torque M_O caused with the resistance against rotation to be proportional to the angular velocity ω_B.

$$M_{BL} + M_{BP} + M_O + M_T + M_E = 0$$
$$-\frac{M_{GL}}{r}l_L + \frac{M_{GP}}{r}l_P - k_\omega \omega_B - J_T\frac{d\omega_B}{dt} - l_T m\frac{d\omega_B}{dt} = 0 \tag{5}$$

where

l_P [m] is distance of the right wheel from point B,

l_L [m] is distance of the left wheel from point B,

l_T [m] is distance of the centre of gravity from point B,

k_ω [kg.m^2.s^{-1}] is resistance coefficient against rotational motion,

J_T [kg.m^2] is moment of inertia with respect to rotation axis in the centre of gravity and

ω_B [s^{-1}] is angular velocity in point B.

The resulting moment of inertia J_B with respect to the rotational axis in the point B is given by Eq. (6) which is the parallel axis theorem or Huygens-Steiner theorem – see e.g. [5].

$$J_B = J_T + ml_T^2 \tag{6}$$

where

J_T [kg.m^2] is moment of inertia with respect to the centre of gravity and

l_T [m] is distance between the centre of gravity and point B.

C. Relationship between Rotation Speed of the Motor and the Centre of Gravity Chassis Movement (kinematics)

The equation describing the behaviour of the two motors (currents and angular velocity) and the behaviour of the chassis (the speed of the linear movement and speed of the rotation) are connected only through torques of motors. Equations of the law of conservation of energy which is conversion of electric energy to mechanical including one type of losses but represent only one relationship between the speed of the two motors (peripheral speed of the drive wheels) and rates of movement and rotation of the chassis. An additional relation is given by design of the drive and chassis. We expect that both drive wheels are firmly linked to rotors of relevant motors over an ideal gearbox with the gear ratio p_G – without nonlinearities and any flexible parts.

The gearbox decreases the output angular velocity ω_{Gx} with relation to the input angular speed ω_x according to the transmission ratio p_G and simultaneously in the same proportion increases output torque M_{Gx} with relation to the input torque M_x.

$$\omega_{GL} = \frac{\omega_L}{p_G} \qquad \omega_{GP} = \frac{\omega_P}{p_G} \tag{7a}$$

$$M_{GL} = p_G M_L \qquad M_{GP} = p_G M_P \tag{7b}$$

Further we assume that both drive wheels have the same radius r and their peripheral speeds v_L, v_P depend on the angular velocity of the gearbox output ω_{GL}, ω_{GP} according to relations

$$v_L = r\omega_{GL} = r\frac{\omega_L}{p_G}$$
$$v_P = r\omega_{GP} = r\frac{\omega_P}{p_G} \tag{7c}$$

To determine the value of the linear speed in the point B and the angular velocity of rotation let us start from Fig. 4. We expect that both drive wheels have the same axis of rotation and therefore their peripheral speeds are always parallel. The illustration shows the positioning where the peripheral speeds v_L and v_P actually operate (driving wheels L and P) and the point B. We want to specify such a linear v_B and angular ω_B speeds that have the same effect as the action of the peripheral speed of the driving wheels. By using the similarity of triangles depicted in Fig, 4 we can recalculate the peripheral speeds of the wheels v_L, v_P to the speed v_B in the point B according to relation (8a) and the angular velocity of rotation ω_B according to the relation (8b).

$$v_B = \frac{v_L l_P + v_P l_L}{l_L + l_P} = \frac{r}{p_G(l_L + l_P)}(l_P\omega_L + l_L\omega_P) \tag{8a}$$

$$\omega_B = \frac{v_B}{x + l_L} = \frac{v_P - v_L}{l_L + l_P} = \frac{r}{p_G(l_L + l_P)}(-\omega_L + \omega_P) \tag{8b}$$

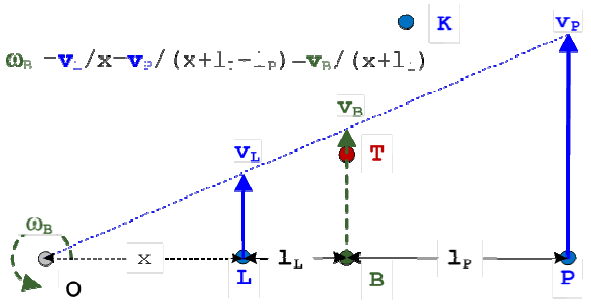

Fig. 4. Linear and angular speeds recalculations.

We can determine from the linear speed of v_B and angular speed ω_B (motion equations) current rotation angle α of the chassis and the current position (the coordinates x_B, y_B) of the point B [7] according to relations

$$\frac{d\alpha}{dt} = \omega_B \tag{9a}$$

$$\frac{dx_B}{dt} = v_B \cos(\alpha) \tag{9b}$$

$$\frac{dy_B}{dt} = v_B \sin(\alpha) \tag{9c}$$

To determine the current position of the contacts of all three chassis wheels (points L, P and K) with ground we need to know the location of these points in relation to the point B. This location is shown in Fig. 5. From geometric dimensions we determine equation describing the relative position of these points in relation to the point B depending on the angle of rotation.

Relative positions Δx_L, Δy_L of the point L and Δx_P, Δy_P of the point P depending on the angle of rotation α are given by

$$\Delta x_L = -l_L \sin(\alpha) \quad \Delta y_L = -l_L \cos(\alpha) \tag{10a}$$

$$\Delta x_P = +l_P \sin(\alpha) \quad \Delta y_P = +l_P \cos(\alpha) \tag{10b}$$

To determine the relative position Δx_K, Δy_K of the point K we use an auxiliary right triangle specified by hypotenuse c and catheti a and l_K (see Figure 5). Then the equations for relative coordinates of the point K calculating are

$$a = \tfrac{1}{2}(l_P - l_L) \quad \gamma = \arctan\left(a/l_K\right) \quad c = \sqrt{a^2 + l_K^2}$$
$$\Delta x_K = -c\sin(\alpha - \gamma) \qquad \Delta y_K = c\cos(\alpha - \gamma) \tag{10c}$$

The dynamic part of the model consists of four differential equations describing the behaviour of both motors, two differential equations describing the dynamics of the chassis and two algebraic equations with dependency of the linear and angular chassis speeds on the peripheral speeds of the driving wheels. We can find in these equations eight state variables describing the current state of the left motor (current i_L, angular velocity of the rotor ω_L, loading torque M_L) and the right motor (current i_P, angular velocity of the rotor ω_P, loading torque M_P) and the movement of the chassis (linear speed v_B and angular velocity of rotation ω_B). All the state variables are dependent on the time courses of the power of the left U_L and right U_P motor.

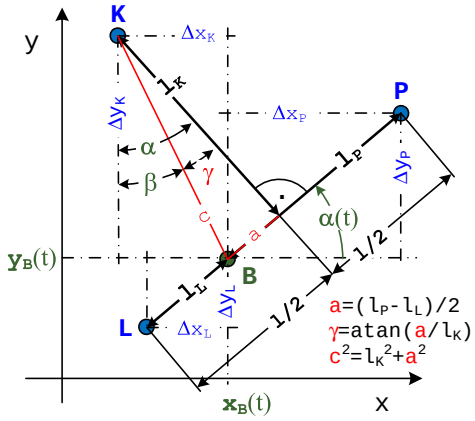

Fig. 5. Arbitrary chassis point recalculation.

Each motor has its own power supply voltage (U_L, U_P) taken from the common source of the voltage U_0. The supply voltage control of both motors using amplifier with the control signal u_x is shown in Fig. 6. Because both motors are powered from the common source it will be taken into account also effect of the internal resistance R_z. Both motors are considered with the same parameters. We can write with using the Eqs. (2) and (3) and Fig. 6 four differential equations describing the behaviour of both motors as

$$Ri_L + R_z(i_L + i_P) + L\frac{di_L}{dt} = u_L U_0 - K\omega_L \tag{11a}$$

$$Ri_P + R_z(i_L + i_P) + L\frac{di_P}{dt} = u_P U_0 - K\omega_P \tag{11b}$$

$$J\frac{d\omega_L}{dt} + k_r\omega_L + M_L = Ki_L \tag{12a}$$

$$J\frac{d\omega_P}{dt} + k_r\omega_P + M_P = Ki_P \tag{12b}$$

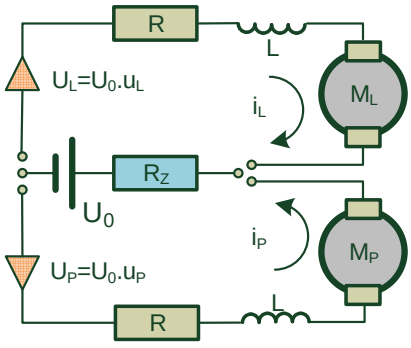

Fig. 6. Motors wiring.

Differential equations (4) and (5) describing the behaviour of the chassis complete the dynamic model. We can rewrite these equations with respect to the equations (7) and introduction of the "reduced" radius of the wheel r_G and total moment of inertia J_B (13a) as

$$r_G = \frac{r}{p_G} \qquad J_B = J_T + ml_T^2 \tag{13a}$$

$$\frac{p_G}{r}M_L+\frac{p_G}{r}M_P-k_v v_B-m\frac{dv_B}{dt}=0$$
$$M_L+M_P-r_G k_v v_B-r_G m\frac{dv_B}{dt}=0 \qquad (13b)$$

$$-l_L\frac{p_G}{r}M_L+l_P\frac{p_G}{r}M_P-k_\omega\omega_B-\left(J_T+ml_T^2\right)\frac{d\omega_B}{dt}=0$$
$$-l_L M_L+l_P M_P-k_\omega\omega_B-r_G J_B\frac{d\omega_B}{dt}=0 \qquad (13c)$$

It is possible to rewrite the last two algebraic equations, (8a) a (8b) describing the dependence between rotation speed of both motors and chassis movement using the substitution (13a) as

$$v_B=\frac{r_G}{l_L+l_P}\left(l_P\omega_L+l_L\omega_P\right) \qquad (14a)$$

$$\omega_B=\frac{r_G}{l_L+l_P}\left(-\omega_L+\omega_P\right) \qquad (14b)$$

These six differential equations (11a,b), (12a,b), (13b,c) and two algebraic equations (14a,b) containing eight state variables representing a mathematical description of the dynamic behaviour of an ideal differentially steered mobile robot with losses linearly dependent on the revolutions or speed. The control signals u_L and u_P that control the supply voltages of the motors are input variables and the speed of the movement v_B and speed of rotation ω_B are output variables. From them with using equations (9a) – (9c) we can determine the current coordinates of the point B and angle of the chassis rotation .

In the following calculation of steady-state values for constant motor power voltages is given. The calculation of the steady-state is useful both for the checking of derived equations and secondly for the experimental determination of the values of the unknown parameters. Because equations. (11)–(14) are linear with respect to the state variables the calculation of the steady-state leads to a system of eight linear equations which we can write in the matrix form as

$$\begin{bmatrix} R+R_z & R_z & K & 0 & 0 & 0 & 0 & 0 \\ R_z & R+R_z & 0 & K & 0 & 0 & 0 & 0 \\ K & 0 & -k_r & 0 & -1 & 0 & 0 & 0 \\ 0 & K & 0 & -k_r & 0 & -1 & 0 & 0 \\ 0 & 0 & 0 & 0 & 1 & 1 & -r_G k_v & 0 \\ 0 & 0 & 0 & 0 & -l_L & l_P & 0 & -k_\omega \\ 0 & 0 & l_P & l_L & 0 & 0 & -\frac{l_P+l_L}{r_G} & 0 \\ 0 & 0 & -1 & 1 & 0 & 0 & 0 & -\frac{l_P+l_L}{r_G} \end{bmatrix} \begin{bmatrix} i_L \\ i_P \\ \omega_L \\ \omega_P \\ M_L \\ M_P \\ v_B \\ \omega_B \end{bmatrix} = \begin{bmatrix} U_L \\ U_P \\ 0 \\ 0 \\ 0 \\ 0 \\ 0 \\ 0 \end{bmatrix} \qquad (15)$$

D. Computational Form of the Model

A mathematical model will be used in particular for the design, simulation and validation of the control movement of the robot. The model can be divided into three series-involved parts as shown in Fig. 7. From the control point of view the action variables are signals u_L and u_P that control the supply voltage of the motors. The instantaneous speed v_B and speed of rotation ω_B are output variables of the linear part of the model. These variables are the inputs to the consequential non-linear part of the model (9a,b,c), whose outputs are controlled variables - the coordinates of the selected point position x_B, y_B and rotation angle of the chassis α. The last part is the calculation of coordinates of the position of arbitrary points of the chassis.

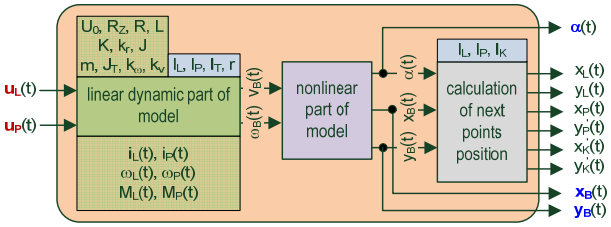

Fig. 7. Model partitioning into linear and nonlinear part.

We can modify the linear part of the model into a simpler form for control design purposes – to reduce number of differential equations from six to four. If we substitute equations (14a,b) into (13b,c) and eliminate torques M_L and M_P by substitution of (12a,b) to (13b,c) we are able to reduce four differential equations (12a,b) a (13b,c) into two (17c,d).

We introduce substitution of the parameters according to following formulas

$$a_L=k_r+\frac{k_v l_P r_G^2}{l_L+l_P} \qquad a_P=k_r+\frac{k_v l_L r_G^2}{l_L+l_P} \qquad (16a)$$

$$b_L=J+\frac{ml_P r_G^2}{l_L+l_P} \qquad b_P=J+\frac{ml_L r_G^2}{l_L+l_P} \qquad (16b)$$

$$c_L=k_r l_L+\frac{k_\omega r_G^2}{l_L+l_P} \qquad c_P=k_r l_P+\frac{k_\omega r_G^2}{l_L+l_P} \qquad (16c)$$

$$d_L=Jl_L+\frac{J_B r_G^2}{l_L+l_P} \qquad d_P=Jl_P+\frac{J_B r_G^2}{l_L+l_P} \qquad (16d)$$

The reduced linear part of the model consists of the set of equations

$$\frac{di_L}{dt}=\frac{u_L U_0-K.\omega_L-(R+R_z).i_L-R_z i_P}{L} \qquad (17a)$$

$$\frac{di_P}{dt}=\frac{u_P U_0-K.\omega_P-(R+R_z).i_P-R_z i_L}{L} \qquad (17b)$$

$$\frac{d\omega_L}{dt}=\frac{1}{b_L d_P+b_P d_L}\left(d_P\left[K(i_L+i_P)-a_L\omega_L-a_P\omega_P\right]-\right.$$
$$\left.-b_P\left[K(-l_L i_L+l_P i_P)+c_L\omega_L-c_P\omega_P\right]\right) \qquad (17c)$$

$$\frac{d\omega_P}{dt}=\frac{1}{b_L d_P+b_P d_L}\left(d_L\left[K(i_L+i_P)-a_L\omega_L-a_P\omega_P\right]+\right.$$
$$\left.+b_L\left[K(-l_L i_L+l_P i_P)+c_L\omega_L-c_P\omega_P\right]\right) \qquad (17d)$$

and the output variables are given by algebraic equations (14a,b).

It is possible to write the reduced linear part of the model as a standard state-space model in the matrix form as

$$\frac{d\mathbf{x}}{dt}=\mathbf{Ax}+\mathbf{Bu} \qquad \mathbf{y}=\mathbf{Cx} \qquad \mathbf{x}=\begin{bmatrix} i_L \\ i_P \\ \omega_L \\ \omega_P \end{bmatrix} \quad \mathbf{u}=\begin{bmatrix} u_L \\ u_P \end{bmatrix} \quad \mathbf{y}=\begin{bmatrix} v_B \\ \omega_B \end{bmatrix} \qquad (18a)$$

with constant matrices **A**, **B** and **C**

$$\mathbf{A}=\begin{bmatrix} -\frac{R+R_z}{L} & -\frac{R_z}{L} & -\frac{K}{L} & 0 \\ -\frac{R_z}{L} & -\frac{R+R_z}{L} & 0 & -\frac{K}{L} \\ \frac{K(d_P+b_P l_L)}{b_L d_P+b_P d_L} & \frac{K(d_P-b_P l_P)}{b_L d_P+b_P d_L} & -\frac{d_P a_L+b_P c_L}{b_L d_P+b_P d_L} & -\frac{d_P a_P-b_P c_P}{b_L d_P+b_P d_L} \\ \frac{K(d_L-b_L l_L)}{b_L d_P+b_P d_L} & \frac{K(d_L+b_L l_P)}{b_L d_P+b_P d_L} & -\frac{d_L a_L-b_L c_L}{b_L d_P+b_P d_L} & -\frac{d_L a_P+b_L c_P}{b_L d_P+b_P d_L} \end{bmatrix}$$

$$\mathbf{B}=\begin{bmatrix} \frac{U_0}{L} & 0 \\ 0 & \frac{U_0}{L} \\ 0 & 0 \\ 0 & 0 \end{bmatrix} \qquad \mathbf{C}=\begin{bmatrix} 0 & 0 & \frac{l_P r_G}{l_L+l_P} & \frac{l_L r_G}{l_L+l_P} \\ 0 & 0 & -\frac{r_G}{l_L+l_P} & \frac{r_G}{l_L+l_P} \end{bmatrix}$$

III. Example of The Behaviour

Basic verification of the above derived model was made by calculation for situations where we can guess the behaviour of the robot. First value of the state variables in steady states will be given for some combinations of parameters and motor supply voltages. Further time courses of the robot trajectory will be determined for some combinations of the time courses of supply voltages when the robot is starting from zero speed.

The values of the parameters listed in the following tables are used in all calculations. These values are chosen so that they at least roughly correspond to the values estimated for the robot in Fig. 1. The values of the geometrical and other parameters of the chassis are listed in Table I.

TABLE I.
Chassis Parameters

Notation	Value	Unit	Description
l_L	0.040	m	distance of the left wheel from point B
l_P	0.060	m	distance of the right wheel from point B
l_T	0.020	m	distance of the centre of gravity from join between wheels
l_K	0.040	m	distance of caster wheel from join between wheels
R	0.050	m	semi-diameter of driving wheel
M	1.250	kg	total mass of the robot
k_v	0.100	kg.s-1	coefficient of the resistance against the robot linear motion
J_T	0.550	kg.m2	moment of inertia of the robot with respect to the centre of gravity
k_ω	1.350	kg.m2.s-1	coefficient of the resistance against the robot rotating

Necessary parameters for the DC motors with common voltage source description are given in Table II. We consider identical motors with identical parameters.

TABLE II.
DC Motors Parameters

Notation	Value	Unit	Description
R	2.000	Ω	motor winding resistivity
L	0.050	H	motor inductance
K	0.100	$kg.m^2.s^{-2}.A^{-1}$	electromotoric constant
R_Z	0.200	Ω	source resistance
U_0	10.00	V	source voltage
J	0.025	$kg.m^2$	total moment of inertia of the rotor and gearbox
k_r	0.002	$kg.m^2.s^{-1}$	coefficient of the resistance against rotating of the rotor and gearbox
p_G	25	---	gearbox transmission ratio

A. Steady State for Different Positions of the Point B and Motors Voltages

The steady states are calculated as a solution of the system of eight equations in matrix form (15). Traces of the wheels are shown during the first 20 seconds of motion from zero initial conditions – calculated from state-space model (18) and from the equations for the trajectories calculation (9, 10).

TABLE III.
Steady State A

	left wheel	right wheel	
u	1.000	1.000	-
l	0.050	0.050	m
i	1.3514	1.3514	A
ω	6.75	6.75	$rad.s^{-1}$
M	0.000001	0.000001	N.m
v_B	0.0013513		$m.s^{-1}$
ω_B	0		$rad.s^{-1}$

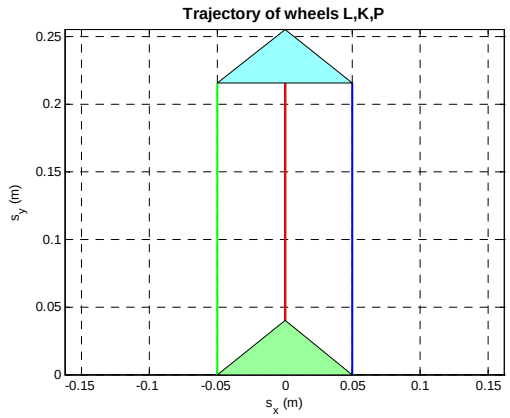

Trajectories are plotted for the situation that the origin of the coordinate system is in the centre between the wheels, which is on the x-axis and the default orientation of the robot is in the direction of the y axis. The starting and final positions of the robot are displayed using the triangle that connects all three wheels. The trajectory of the centre of gravity is displayed (red colour) in addition to the traces of the wheels.

The steady-state A (Table III.) corresponds to the geometric arrangement – the point B is midway between the wheels and both motors have the same supply voltage. The result is that the robot moves only linearly.

The following three experiments show the influence of the centre of gravity position.

The steady-state B (Table IV.) holds again for the symmetric geometric arrangement but only one motor is powered.

The steady state C (Table V.) shows the situation in the case that the point B is in the extreme position towards the left wheel and only the left motor is powered.

The steady-state D (Table VI.) corresponds to the same position of the point B towards the left wheel but only the right motor is powered.

In all three cases the robot rotates and at the same time the point B has some linear speed. Both wheels produce translational movement because of the interactions.

TABLE IV.
STEADY STATE B

	left wheel	right wheel	
U	0.000	1.000	-
L	0.050	0.050	m
I	-0.2772	1.6287	A
ω	0.2842	6.7818	rad.s^{-1}
M	-0.001176	1.03010	N.m
v_B	0.006757		m.s^{-1}
ω_B	0.7776		rad.s^{-1}

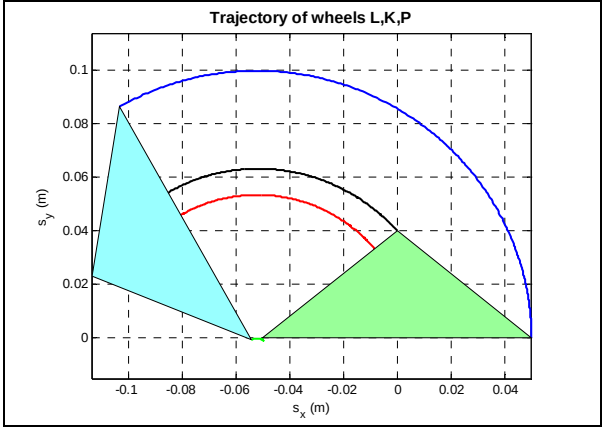

TABLE V.
STEADY STATE C

	left wheel	right wheel	
u	1.000	0.000	-
l	0.000	0.100	M
i	1.6288	-0.2773	A
ω	6.4721	0.2842	rad.s^{-1}
M	0.00334400	-0.00334141	N.m
v_B	0.0129441		m.s^{-1}
ω_B	-0.7776		rad.s^{-1}

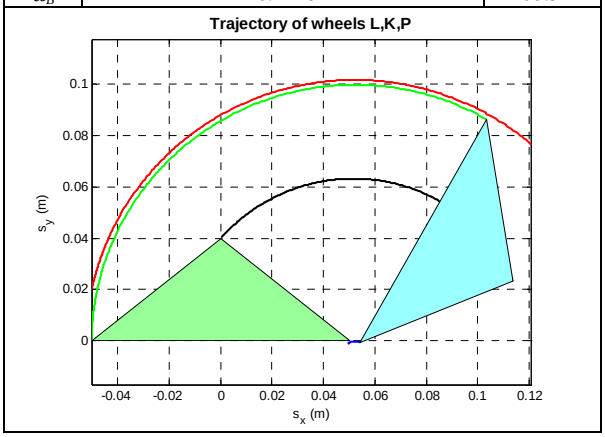

TABLE VI.
STEADY STATE D

	left wheel	right wheel	
u	0.000	1.000	-
l	0.000	0.100	M
i	-0.2773	1.6286	A
ω	0.2842	6.4721	rad.s^{-1}
M	-0.00334148	0.00334159	N.m
v_B	0.0005686		m.s^{-1}
ω_B	0.7776		rad.s^{-1}

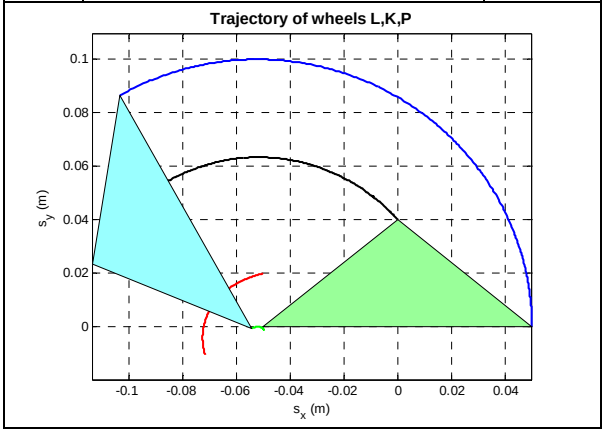

B. Dynamic Behaviour for Particular Cases

The dynamic behaviour is demonstrated on the time courses of currents and angular speeds of the motors starting from zero initial conditions. Graphs in Fig. 8 show courses of the supply voltages, currents and angular speeds for the case that the point B is in the middle between both motors with the same constant voltage 10 V. The situation corresponds to experiment with the parameters in Table III.

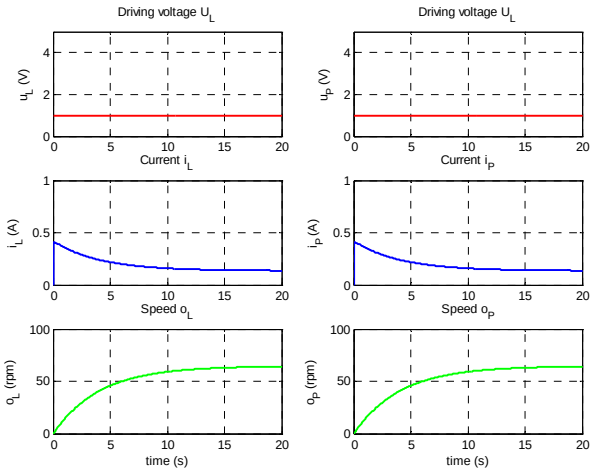

Fig. 8. Dynamic behaviour – constant supply voltage 10 V for both motors.

A situation where the point B is in the middle between both motors with the right motor voltage 10 V only corresponds to the experiment with the parameters in Table IV. and it is demonstrated in Fig. 9.

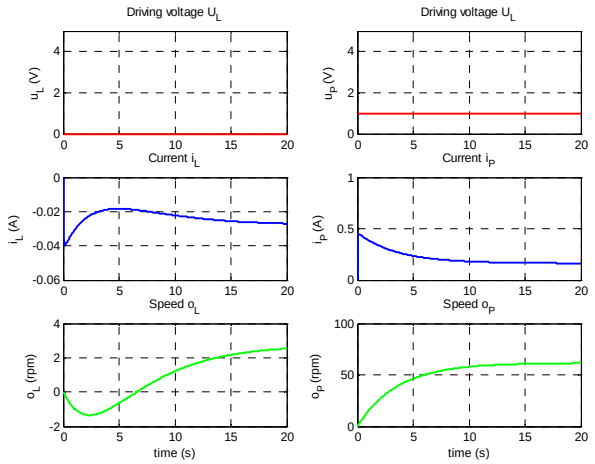

Fig. 9. Dynamic behaviour – constant supply voltage 10 V for right motor.

An illustrative example of behaviour in the situation when both voltages are periodic and with different amplitudes is in Figs. 10 and 11.

On the left motor a rectangular train of pulses with period 20 s, duty cycle 50 % and amplitude 3 V is applied. On the right motor a rectangular train of pulses of doubled period 40 s and amplitude 4 V is applied.

The corresponding vehicle motion – wheels trajectories – is in Fig. 11.

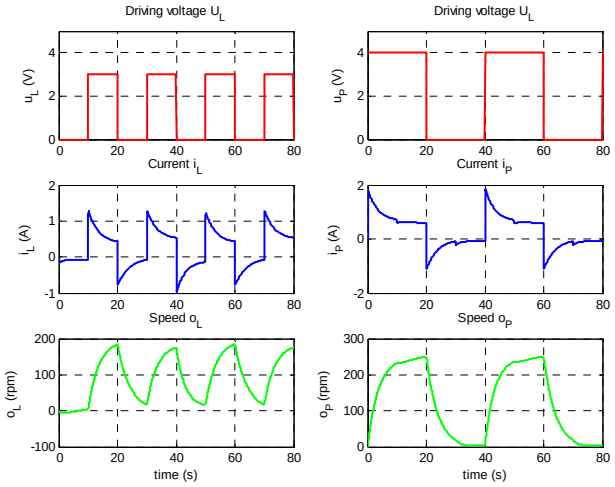

Fig. 10. Dynamic behaviour – periodic voltages.

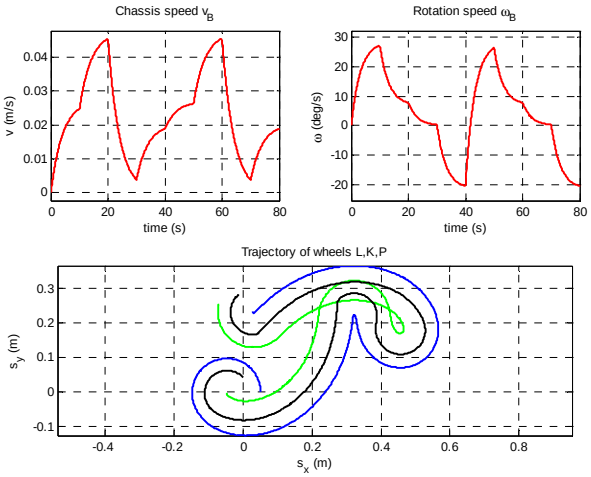

Fig. 11. Dynamic behaviour – periodic voltages – speeds and trajectories.

IV. Conclusions

The behaviour of the dynamic model in the simulated situations agrees with the expected behaviour of the robot. The position of the centre of gravity does not affect the behaviour in steady state. The immediate linear speed in the point B depends on its position but the trajectories of the wheels are independent on the position of the point B.

The interaction of the two drives was confirmed. The wheel without supply voltage rotates, because of the forces of inertia and the forces of resistance. In the transient state, this can cause change in direction of the wheel rotation. This situation is seen in Fig. 9.

Motor dynamics is negligible compared with the expected dynamics of the chassis for the estimated motor parameters. Because the parameters of the model have physical meaning it will be possible to measure directly some parameters on a real device. The identification of additional parameters will be possible experimentally from the measured time courses of power voltages and corresponding courses of angular speed of the wheels.

Acknowledgment

This research was supported by Institutional support of The Ministry of Education, Youth and Sports of the Czech Republic.

References

[1] P. Novák, *Mobilní roboty (pohony, senzory, řízení)*. BEN 2005, ISBN 80-7300-141-1.

[2] R.F. Stengel, *Robotics and Intelligent Systems; A Virtual textbook*, http://www.princeton.edu/~stengel/RISVirText.html [cited 11.11.2010].

[3] G.W. Lucas, *A Tutorial and Elementary Trajectory Model for the Differential Steering System of Robot Wheel Actuators*, http://rossum.sourceforge.net/papers/DiffSteer/DiffSteer.html [cited 11.11.2010].

[4] Z. Winkler, *Odometrie*; http://robotika.cz/guide/odometry/cs [cited 11.11.2010].

[5] Z. Horák, F. Krupka, *Fyzika*, vol. 1. SNTL Praha, 1976, pp. 422.

[6] F. Poliak, V. Fedák, L. Zboray, *Elektrické pohony*, Bratislava: Alfa, 1987.

[7] J. Šrejtr, *Technická mechanika II. Kinematika 1. část.* SNTL Praha, 1954, pp. 256.